Fibrilization



Improved Intervarn Friction, Impact Response, and Stab Resistance of Surface Fibrilized Aramid Fabric

Jalal Nasser, Kelsey Steinke, LoriAnne Groo, and Henry A. Sodano*

Improvement of the ballistic performance of aramid fabric is an important topic in the study of soft body armors, especially with their increasing use in such applications over the past decades. To enhance and tailor the performance of fabrics, having control over one of its primary energy absorption mechanisms, intervarn friction, is required. Here, a recently reported surface fibrilization method is exploited and optimized to improve intervarn friction in aramid fabrics. Through tow pullout testing of fibrilized fabrics, the fibrilization treatment is shown to provide up to seven times higher pullout energy and six times higher peak load. To correlate the effects of the treatment on the ballistic response, impact tests are conducted on treated fabric targets using a gas gun setup. The fibrilized fabrics displayed a 10 m s⁻¹ increase in V_{50} velocity, compared to that of untreated fabrics, while retaining its original flexibility and mechanical strength. Similarly, the fibrilization treatment also resulted in 230% improvement in depth of penetration when dynamically stabbed using a spike impactor. The results demonstrate the potential of the proposed surface fibrilization treatment as a fast and cost-effective technique to improve the ballistic and stab performance of aramid-based soft body armors.

1. Introduction

With the development of high-tenacity polymer fibers in the 1960s, highly impact-resistant fabrics have been introduced into a wide range of ballistic applications, such as soft body armors, commercial aircraft, and armor plating of military vehicles to provide protection against blasts, projectiles, and fragments.^[1–3] Polymeric woven fabrics, such as aramid (Kevlar, Twaron) and ultrahigh molecular weight polyethylene (Dyneema, Spectra), have been popular choices for ballistic impact protection

J. Nasser, L. Groo, Prof. H. A. Sodano
Department of Aerospace Engineering
University of Michigan
Ann Arbor, MI 48109, USA
E-mail: hsodano@umich.edu
K. Steinke, Prof. H. A. Sodano
Department of Materials Science and Engineering
University of Michigan
Ann Arbor, MI 48109, USA
Prof. H. A. Sodano
Department of Macromolecular Science and Engineering
University of Michigan
Ann Arbor, MI 48109, USA

The ORCID identification number(s) for the author(s) of this article can be found under https://doi.org/10.1002/admi.201900881.

DOI: 10.1002/admi.201900881

because of their lightweight and flexibility as well as their high specific strength and tensile tenacity.^[4,5] With a specific energy absorption six times that of an aluminum fuselage skin, aramid fabrics enable lowdensity materials with high-performance ballistic energy dissipation.[6,7] Beyond the fiber properties, the structure of the woven fabric also imparts energy absorption properties that are typically derived from the weave architecture of the fabric, varn crimp, and interfacial interactions between the constituent fibers and tows.^[6] However, while polymeric fabrics have almost completely replaced conventional materials in certain body armor equipment, such as combat helmets, [8] bulletproof vests still require the use of metallic or ceramic components for adequate ballistic protection, thus increasing the weight of the armor and reducing the user's mobility.[9,10] Moreover, the weak resistance of the aramid fabric to sharp piercing objects, such as knives, makes it

unsuitable for use as stab protection.^[11,12] Therefore, in order to maximize the benefits of using aramid fabrics in ballistic applications, it is necessary to improve its impact resistance while maintaining its flexibility and lightweight.

Various studies have been conducted to improve the ballistic performance of dry woven aramid fabrics, ranging from numerical analysis and modeling to experimental studies and mechanical testing. The effects of multiple fabric parameters on impact response have been investigated, including the number of fabric plies and their stacking sequence, fabric architecture, intervarn friction, operating temperatures, and projectile characteristics. By accounting for the contact between adjacent plies of a target, the numerical model proposed by Ting et al. demonstrated an improved ballistic performance with increased friction slippage at yarn crossing points.[13] Such results indicate the importance of intervarn friction as an energy dissipation mechanism of impact-loaded woven fabrics. Experimentally, the energy absorption of the fabric was found to be roughly proportional to the areal density but not to the mesh density or weave tightness.^[14] Hybrid fabrics composed of a combination of Kevlar and carbon fiber were also found to exhibit superior ballistic performance, [15] while the difference in the performance of the plied versus spaced configuration was concluded to be dependent on the geometry and application of the projectile used. [16,17] Other studies focused on the effects of fiber twist and yarn crimp



on the ballistic performance of the fabric. Rao et al. optimized the tensile strength of fibers through twist angle of 7°,[18] while Chitrangad reported improvement in the limit velocity required for a projectile to penetrate target fabrics, known as the V_{50} speed, when hybridized weaves were designed for simultaneous failure of weft and warp yarns.[15] By replacing the original weft yarns with ones possessing larger elongation, the effect of varn crimp was mitigated, and varn undulation was reduced. Moreover, low-temperature operating conditions were also found to be ideal for the energy absorption performance of fabrics such as Dyneema and Kevlar 29, as increasing temperatures led to a decrease in the elastic modulus of the fiber.[19] Finally, projectile properties, such as geometry and mass, [14] angle of incidence, [20] and point of impact,^[21] were all also found to have significant impact on the ballistic performance and energy dissipation mechanisms of a woven fabric.

One of the most important and widely studied energy dissipation mechanism in the impact response of woven fabrics is intervarn friction. The mobility and friction between fabric varns during impact is a primary energy dissipation mechanism, as it directly correlates to the fiber-fiber interfacial properties of the fabric. Recently, many fiber surface modification techniques, such as lubrication, [22,23] coatings, [24–26] and interphase design, [27,28] have been proposed to improve impact response through increased interyarn friction. Dischler reported superior distribution of ballistic energy of aramid fabrics with the intervarn friction improving by a 2 µm pyrrole thick coating applied to aramid fibers. [29] Moreover, Chitrangad developed a fluorinated finish for aramid fibers that increases intervarn friction.[30] However, such finishing was found to be incompatible with water-repellant agents, leading to increased slippage of the bullet between yarns and lower intervarn friction force in wet fabrics.[31,32] Impregnating Kevlar fabric with colloidal shear thickening fluids was also reported as an applicable method to improve ballistic performance through reduced yarn mobility. Lee et al. reported improved impact resistance at higher strain rates with no loss of fabric flexibility by the use of colloidal shear thickening fluids. The improved properties at high strain rates were attributed to the transfer of loading concentration from the primary yarns into the entirety of the aramid fabric.[33] However, shear thickening fluids fail to provide any impact protection at lower strain rates or against stabbing attacks.^[34] The use of ethylene/methyl acrylate copolymer coatings to improve the intervarn friction was also studied by Gawandi et al. It was reported that by hot pressing the polymer-coated fabric, transverse infiltration of the polymer coating into yarn crossing sections is achieved, and a 124% increase in tow pullout peak load was observed.^[35] The improvement to the ballistic performance of the fabric obtained using the discussed surface modification techniques confirms the important role of interfacial properties in the impact response and behavior of aramid fabrics.

Recently, interphase design has been extensively used as an interface reinforcing technique in woven fabrics and fiber reinforced composites. By grafting nanomaterials onto the surface of the fiber, the mobility of both fiber and tows is decreased, and the sliding friction between yarns is increased.^[27,28]

Obradović et al. demonstrated improved ballistic performance in aramid composites through the addition of silica nanoparticles to its surface. [36] Labarre et al. also showed a 230% increase in varn pullout peak load by grafting multiwall carbon nanotubes onto the surface of aramid fibers. [25] However, the grafting methods used, such as chemical vapor deposition (CVD), required high operating temperatures that are incompatible with polymer fibers. The development of novel hydrothermal growth methods of vertically aligned ZnO nanowires has allowed the ability to benignly graft nanomaterials on the surface of aramid fibers without any degradation of the fibers.^[37,38] Galan et al. reported a 228% improvement in the interfacial strength of carbon fiber reinforced composites with optimized ZnO nanowires grafted to the surface of the fiber.^[39] Hwang et al. also showed the ability to tailor the interyarn friction of ZnO nanowire coated aramid fabrics through control of the nanowire morphology, and observed up to 22.7 times higher energy absorption than that of a untreated fabric.^[40,41] Moreover, Malakooti et al. reported a 66% increase in impact resistance of ZnO nanowire coated aramid fabrics compared to that of untreated fabric, when subjected to intermediate velocity impact tests.^[42] The improvement in impact response was explained to be a result of the increase in mechanical interlocking and contact area between neighboring aramid fibers.[43,44]

Alternatively, Nasser et al. reported a fibrilization technique of aramid fabric using a basic solution to form pseudo-wiskerized aramid fibers. [45] The treatment also increased surface polar functional groups, providing a combination of improved chemical interaction and mechanical interlocking as a reinforcement mechanism. The fibrilized fibers possessed a 128% improved interfacial shear strength with the epoxy matrix, while also preserving the tensile strength of the fibers. In this study, the fibrilization process was optimized to achieve improved intervarn friction and ballistic performance in aramid fabrics. The effect of fibrilization on the intervarn friction of aramid fabrics was studied using tow pullout testing. Additionally, the impact response was investigated through measurement of V_{50} speeds using an instrumented gas gun system, while stab resistance was characterized using dynamic drop tower and quasistatic stab testing. Accurate measurement of the projectile's velocity allowed for proper assessment of the effect of fibrilization on the ballistic performance of aramid fabrics. Untreated aramid fabrics were also subjected to tow pullout, ballistic, and stab testing for reference. The tow pullout peak load and V_{50} speeds were found to increase by more than 500% and 10 m s⁻¹, respectively, in fibrilized aramid fabrics. Inversely, the depth of spike impactor's penetration was observed to decrease by 230% in treated fabrics. Finally, the failure modes during all tests were investigated using scanning electron microscopy (SEM) in order to gain further insight on the fibrilization process's role in interfacial reinforcement during pullout, impact, and stab loading.

2. Results and Discussion

The effect of the fibrilization process on the surface morphology of the fibers is confirmed through the SEM images as

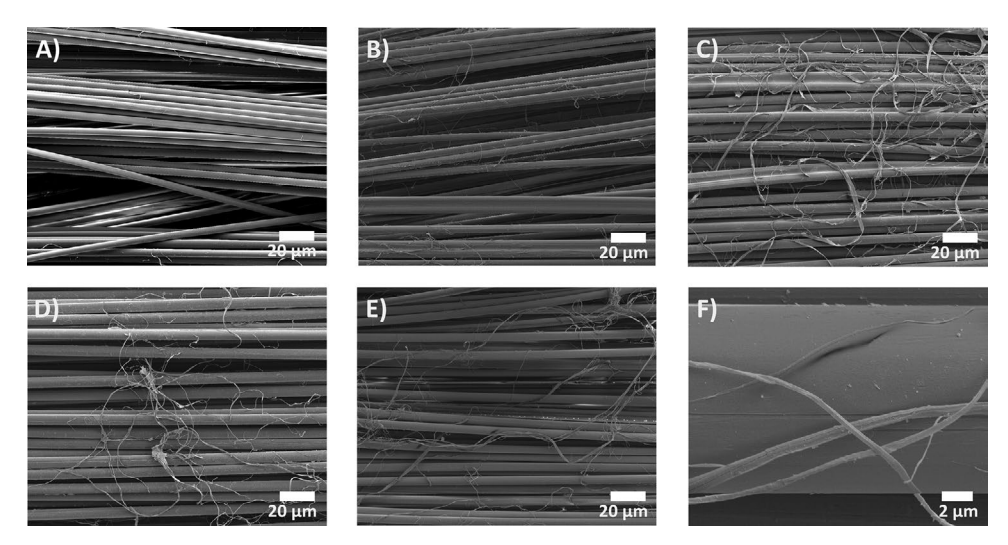


Figure 1. Scanning electron microscopy images of the untreated and the treated fibers. A) Untreated fibers and B) fibers after a 2 h treatment. C) Fibers after a 5 h treatment. F) Fibers after a 7 h treatment. E) Fibers after a 10 h treatment. F) Generated fibrils.

shown in Figure 1. The deprotonation of the macroscale fibers inside the basic solution generates randomly oriented aramid fibrils with varying aspect ratios and diameters. Shorter treatment periods were previously found to reduce the breakage of interchain hydrogen bonds, allowing for a larger amount of the newly formed fibrils to remain attached to the macroscale fiber surface. The presence of these fibrils has been shown to improve the mechanical interlocking capacity of aramid fabrics with polymers such as epoxy at the level of the fibermatrix interface.^[45] High aspect ratio fibrils can be seen spanning across multiple fibers and at crossing points of tows in both weft and warp direction. Such fibrils can help enhance the impact resistance against bowing of the aramid fabric by bridging between neighboring fibers and forming interfiber structures. These interfiber structures can also largely increase the interyarn friction in the fabrics by introducing stronger mechanical interlocking. Moreover, the fibrilized aramid fabrics exhibited no increase in weight or decrease in flexibility, thus preserving important characteristics of aramid fibers for its ballistic performance.

2.1. Tensile Strength

The superior ballistic performance of aramid fabrics is partially attributed to its high tensile properties. Nilakantan et al. reported direct correlation between the ballistic performance of woven fabric and its corresponding yarn tensile strength, where a decrease in mean strength of the yarn resulted in reduction of fabric's V_{50} velocity. Therefore, the enhancement of the interyarn friction of the aramid fabric should not come at the expense of the individual strength of the fiber or fabric. To ensure no degradation of tensile properties of aramid fabrics occurs during fibrilization, textile fabric and single fiber tensile testing of untreated and treated samples is performed at quasistatic tensile loading. The elastic modulus and tensile strength of untreated and fibrilized single aramid fibers can be seen in **Figure 2**A,B. No significant statistical decrease in the

tensile strength of fibrilized aramid fibers is observed until a minimum treatment period of 10 h. The tensile strength and elastic modulus of aramid fibers treated for 10 h are found to decrease by 8.9% and 9.5%, respectively. This trend is confirmed by the further decrease in tensile properties of fibers treated for 24 h, where a decrease of 12.6% in the tensile strength is observed. The degradation of the aramid fiber's strength at longer treatment periods is due to the prolonged deprotonation and hydrolysis process occurring inside the basic fibrilization solution. The effect of fibrilization is further studied through measurement of the tensile properties of both untreated and fibrilized aramid fabrics according to ASTM D5353 (Figure 2C,D). Similar to single fiber tensile testing, a 7.5% and 6.8% decrease in tensile strength and elastic modulus, respectively, is observed in aramid fabric treated for 10 h. The expected decrease in the tensile properties of the fabric is due to weakened yarn and individual fiber strength, thus indicating that treatment periods longer than 10 h will be expected to offer no reinforcement to the ballistic performance of the aramid fabric. It should be noted that the slight increase in tensile strength of fabrics treated for 5 h can be caused by the potentially increased intervarn friction between the tows. It can then be concluded that the tensile strength of aramid fabrics is fully preserved for fibrilization treatment periods of less than 10 h, and its ballistic performance is not at risk of decreasing within that range.

2.2. Interyarn Friction

To investigate the effect of the fibrilization treatment on the energy absorption capacity of the aramid fabrics, single tow pullout testing is performed under controlled transverse tension using the experimental setup shown in **Figure 3**. The load–displacement curves are recorded at the same preload transverse tension of 100 N. The amount of energy absorbed during pullout, known as the pullout energy, is calculated through integration of the recorded load–displacement curves. By testing

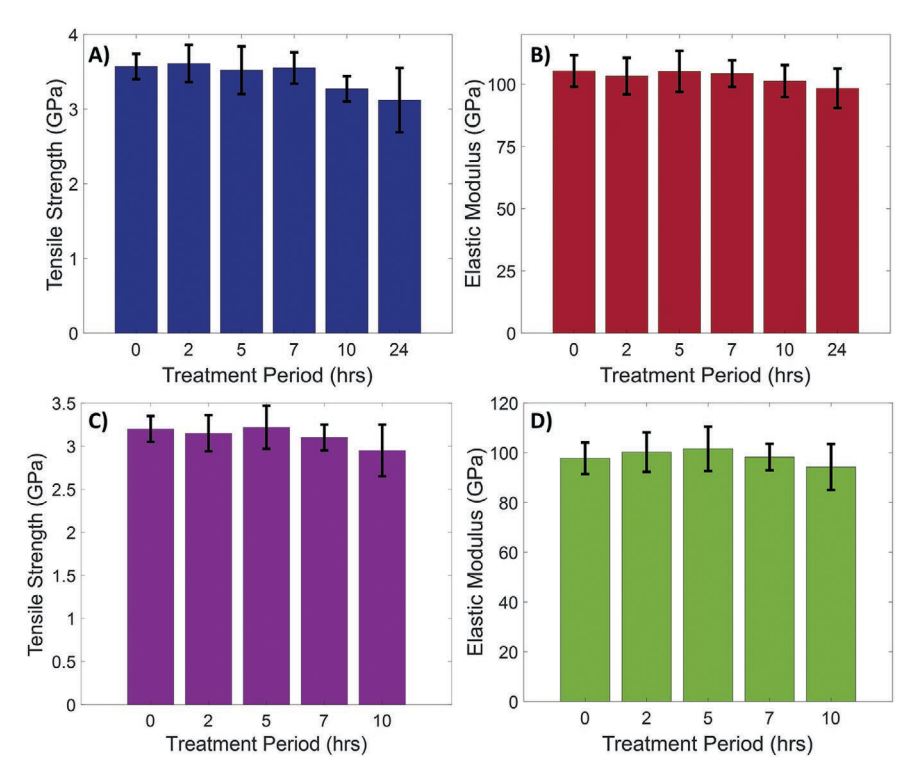


Figure 2. A) Tensile strength of the untreated and the treated single aramid fibers for various durations. B) Elastic modulus of the untreated and the fibrilized single aramid fibers for various durations. C) Tensile strength of the untreated and the fibrilized aramid fabric for various durations. B) Elastic modulus of the untreated and the fibrilized aramid fabric for various durations.

seven tows per fabric, the uniformity of the fibrilization treatment and the repeatability of the tow pullout testing process are ensured. The averaged pullout energy of the untreated and fibrilized fabrics is listed in **Table 1**, and the peak loads along with the corresponding load–displacement curves are shown in **Figure 4**. Both pullout load and pullout energy are increased by more than 157% and 194%, respectively, after only 2 h of fibrilization treatment. A maximum increase in pullout properties

is found in fibrilized aramid fabric with a treatment period of 5 h which shows an increase of 550% and 665% in peak load and pullout energy, respectively. By studying the recorded peak load-displacement curves, it can be seen that the loaded tow initially experiences static friction, highlighted by the first recorded peak. This is followed by a large drop in the load as the specimen undergoes kinetic friction when passing through the first transverse tow. The increase in static friction before uncrimping is attributed to the improved mechanical interlocking between fibrilized fibers, indicating increased intervarn friction. Further decrease in load along with certain local peaks are recorded as the loaded tow passes through all remaining transverse tows. Moreover, fibrilized aramid fabrics display slightly larger extensions before complete pullout, resulting in further enhancement of the pullout energy. The observed delay in pullout failure confirms larger resistance to yarn pullout stemming from the improved interaction between the neighboring and intersecting tows of the fibrilized aramid fabric. Such pullout behavior agrees well with that of other cases of aramid fabric

treatment methods reported in previous studies, such as polymeric and ZnO nanoparticle coatings.^[42] By performing an examination of tow pullout samples using SEM imaging following the completion of the test, dense bundles and layers of dispersed fibrils and fibrilized aramid fibers can be seen at the yarn-crossing points of 5 and 10 h treated aramid fabrics, whereas untreated fabrics display no sign of excessive fibrilization (**Figure 5**). As expected, the degree of fibrilization in 5 h

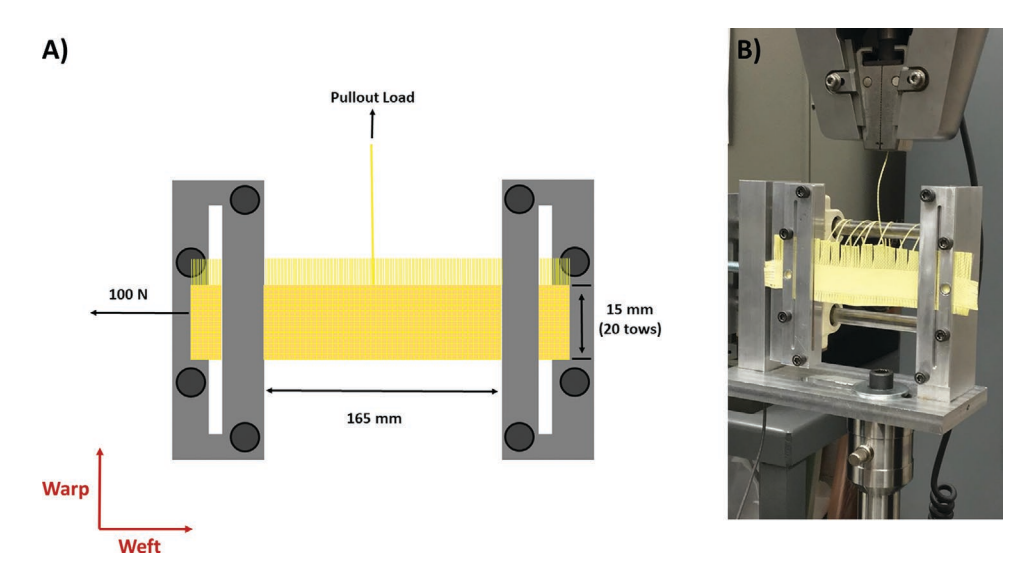


Figure 3. A) Schematic of experimental setup for tow pullout test. B) Treated aramid fabric sample for tow pullout.

Table 1. Averaged pullout energy and peak load of untreated and treated fabrics.

Treatment period [h]	0	2	5	7	10
Pullout energy [mJ]	4.18	12.32	32.93	22.45	23.43
Standard deviation	0.91	1.39	3.29	2.01	1.87
% Improvement	-	194.4	665.3	437.3	460.2
Peak load [N]	0.89	2.29	5.79	4.75	4.63
Standard deviation	0.17	0.32	0.62	0.54	0.75
% Improvement	_	157.3	550.5	433.7	420.2

treated fabric is considerably larger than that in a 10 h treated sample, further confirming the tow pullout results. The abrasive loading experienced during a tow pullout generates aramid surface fibrils in both the untreated and treated case due to the breakage of the hydrogen bonds responsible for holding individual polyamide macromolecules together; however, the deprotonation process to which the aramid fabric is subjected further weakens hydrogen bonding, promoting easier fibrilization of the treated surface of the aramid fibers under abrasive action. Therefore, the increased surface fibrils found in treated fabrics post-testing can be attributed to both the initial fibrilization treatment, and the breakage of hydrogen bonding during abrasive loading. The presence of these microstructures indicates an increase in intervarn friction by means of mechanical interlocking, resulting in the observed improvement in initial peak load and pullout energy of the fabric. Thus, the preservation of tensile strength and the considerable enhancement to the intervarn friction of aramid fabrics after short treatment periods show its ability to translate into a higher impact resistance, yielding the desired characteristic of improved ballistic performance. It should also be noted that the improvement in intervarn friction saturates, as 7 and 10 h treatments only show a 20.4 and 24.54% decrease in pullout energy when compared to that of a 5 h treatment, respectively. Regardless, these set of fibers still possess a minimum 437% higher pullout energy than that of untreated fabrics. The reason for such a trend is the decrease in fibril density on the macroscale aramid fiber's surface since the fibrils generated at early treatment stages start to debond, lowering the effectiveness of the mechanical interlocking due to the treatment. These observed trends are unique to the treatment conditions of this study, as the use of different bases and concentrations may alter the rate of the deprotonation process.

2.3. Impact Response

The influence of fibrilization on the impact resistance of aramid fabrics is evaluated by subjecting the treated fabrics to impact tests at velocities ranging from 75 to 115 m s⁻¹. The tested fibrilized aramid fabrics are treated for 5 h for the optimized ability to maintain the tensile strength of both the aramid fiber and fabric, while yielding maximum improvement in intervarn friction. The treated fabrics are tested over three different velocity zones before calculating the V_{50} speed. The V_{50} speed is considered a reliable criterion for quantification of the impact resistance of woven fabrics, as it represents the speed limit up to which the target is impenetrable by a specific projectile. Proper clamping of the samples from all sides is necessary to avoid slippage which can result in inaccurate impact responses. Penetration of the fabric is considered to be successful in the case where the projectile is able to impact the clay trap placed 2 in. behind the fabric target. The projectile's velocity for each performed test along with the type of failure across all velocity zones are presented in **Table 2**. At speeds less than 88 m s⁻¹, both untreated and treated aramid fabrics are able to stop the projectile, dissipating all its kinetic energy and preventing it from penetrating and reaching the clay trap. However, as projectile's

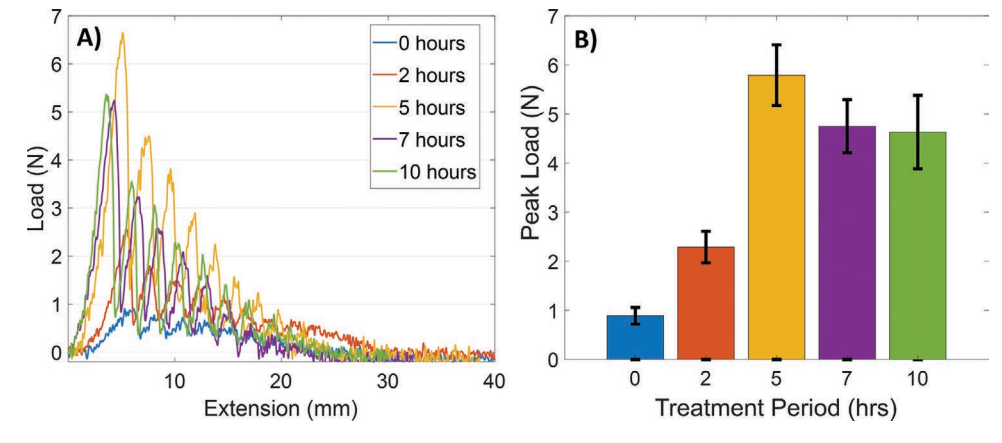


Figure 4. A) Load-displacement curve showing tow pullout behavior of different treatment periods. B) Comparison of average peak load values between the samples.

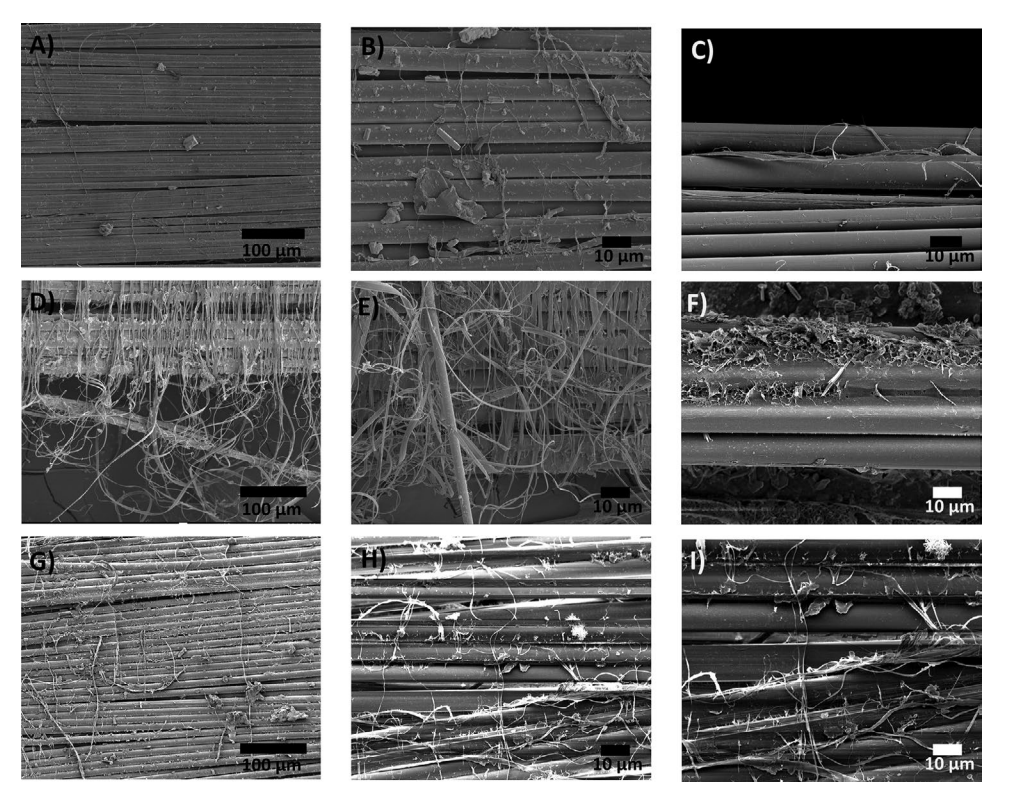


Figure 5. SEM images of aramid fabrics, both untreated and treated, after pullout test at yarn-crossing points: A–C) untreated, D–F) 5 h treated fabric, and G–I) 10 h treated fabric.

velocity is increased into the intermediate range of 88–98 m s⁻¹, the impactor is able to penetrate untreated aramid fabrics at certain speeds but not the treated fabric. The higher impact resistance observed in the treated aramid fabric is the result of the improved energy dissipation mechanisms due to the fibrilization. The treated fabric's increased interyarn friction leads to a limited mobility of neighboring fibers and tows which

Table 2. Details of all the reported impact tests for untreated and treated aramid fabrics.

Untreated ara	mid fabric	Fibrilized fabric		
Impact speed [m s ⁻¹]	Failure	Impact speed [m s ⁻¹]	Failure	
79.37	No penetration	87.69	No penetration	
81.32	No penetration	90.79	No penetration	
83.23	No penetration	95.29	No penetration	
87.72	No penetration	97.23	No penetration	
88.60	Penetration	98.25	Penetration	
90.07	No penetration	99.21	Penetration	
92.96	Penetration	100.26	No penetration	
93.75	No penetration	101.6	Penetration	
95.25	Penetration	102.82	Penetration	
97.60	Penetration	103.58	No penetration	
99.73	Penetration	104.09	No penetration	
102.97	Penetration	105.83	Penetration	
112.34	Penetration	108.62	Penetration	

decreases the possibility of wedge-through projectile penetration due to bowing. Moreover, the treated fabric visibly exhibits no more local or remote yarn failure, given both possess similar tensile strengths. As the velocity is further increased to over 97 m s⁻¹, complete penetration of the projectile starts to occur in treated fabrics. At such speeds, the aramid fabric is unable to absorb all of the projectile's kinetic energy as penetration occurs and the projectile's momentum was stopped by the clay trap. The calculated V_{50} of the treated aramid fabric is found to be ≈ 10 m s⁻¹ higher than that of untreated fabric, indicating an improved impact response due to fibrilization. The observed 12% improvement in V_{50} speed of treated aramid fabrics predictably agrees well with the previously discussed 550% increase in yarn pullout force. The limited improvement in ballistic performance relative to that of intervarn friction is mainly due to the contribution of multiple failure mechanisms to the failure of the fabric under impact loading conditions. The high strain rate loading conditions of impact testing are shown to excite p-phenylene terephthalamides (PPTA) bonds beyond their activation energy, resulting in primary bonds breakage and the promotion of brittle fracture. [47] The ability of aramid yarns to withstand rupture is independent of any interfacial properties, as it is primarily dictated by fiber and yarn's tensile properties. Therefore, the contribution of these other failure modes limits the effect of interfacial reinforcement on the impact resistance of aramid fabrics.

Examining the failure modes of untreated and treated aramid fabrics through post-testing imaging allows for accurate interpretation of the role of the fibrilization treatment in the

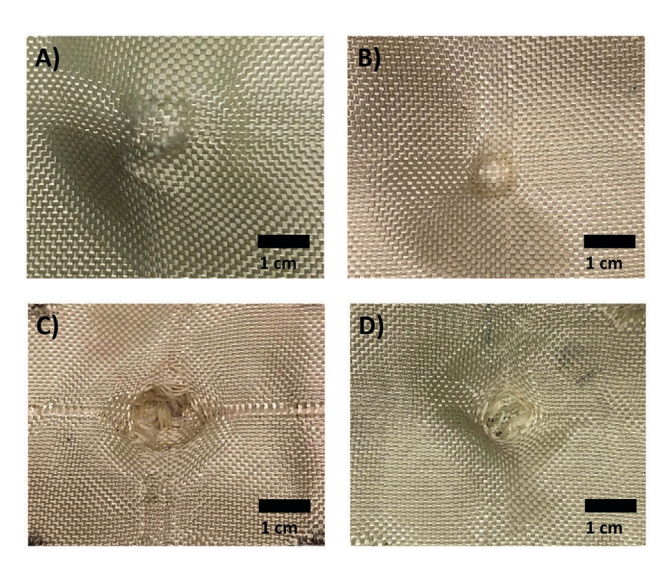


Figure 6. Comparison between untreated aramid fabrics and treated aramid fabrics (bottom row) after impact: A) untreated aramid fabric after low velocity, nonpenetrating impact (below 90 m s $^{-1}$); B) treated aramid fabric after low velocity, nonpenetrating impact (below 90 m s $^{-1}$); C) untreated aramid fabric after high velocity, fully penetrating impact (above 100 m s $^{-1}$); D) treated aramid fabric after high velocity, fully penetrating impact (above 100 m s $^{-1}$).

impact resistance reinforcement mechanism. At lower speeds, the projectile is unable to penetrate the target but still resulted in deformations to the fabric. In comparison to treated fabric, the untreated fabric experiences larger deformations around the blast area due to bowing along with further damage to the second and third ply, as the first one absorbs less kinetic energy than in the case of the treated fabric. The difference in bowing behavior correlates to the mobility of the tows and fibers within the fabric. As full penetration starts to occur at higher projectile speed, the failure mode of the aramid fabrics is modified. The ability of adjacent yarns and fibers in untreated fabric to easily slide results in traces of yarn pullout around the blast area as

well as a cross-shaped yarn pullout (Figure 6) due to the foursided clamping of the sample. Significantly less yarn pullout/ sliding is observed in treated fabrics due to the increased intervarn friction and decreased varn mobility through the generated surface fibrils. Moreover, the blast hole left by the penetrating projectile is significantly smaller in treated fabrics than untreated ones, signaling a decrease in the ability of the projectile to wedge through the fabric's yarns. It should be noted that both sets of fabric experience a high degree of remote and local yarn rupture which can be considered as the primary failure mechanism at such high speeds. SEM images of the blast area of untreated and treated fabric targets can be seen in Figure 7. Post-testing, untreated aramid fabrics are found to sustain substantial deformation around the blast area as the projectile velocity is increased. The deformation in untreated fabric is primarily in the form of yarn sliding and weave distortion, as no excessive signs of surface fibrillation are found. However, even at high projectile velocities, treated fabrics display minimal yarn sliding and weave deformation, yet surface fibrillation is prominent. Moreover, both fabrics present structural failure in the form of the ruptured fibers as seen in Figure 7. The observed difference in failure mechanisms agrees well with the V_{50} metrics detailed in Table 2. These results confirm the ability of the increased intervarn friction achieved through fibrilization treatment to contribute into an improved impact response of aramid woven fabrics.

2.4. Stab Resistance

The capacity for fibrilized aramid fabric to improve stab protection against a spike is studied by performing drop tower testing on treated targets from a fixed height with varying drop masses. Similar to ballistic testing, eight aramid fabric plies are treated for 5 h and used as impact targets. The fibrilization treatment has no considerable effect on the areal density, thickness, or flexibility of the aramid fabric, and therefore the same number of plies was used for both untreated and treated fabric targets

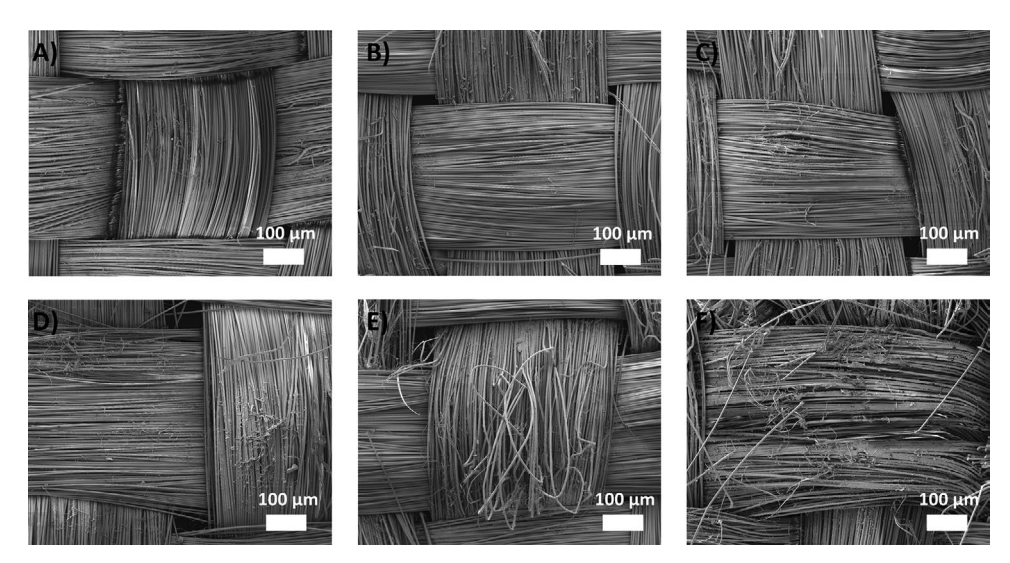


Figure 7. Images of aramid fabrics after impact testing: A,B) Untreated and treated aramid fabric tested at 87 m s⁻¹, respectively. C,D) Untreated and treated aramid fabric tested at 95 m s⁻¹, respectively. E,F) Untreated and treated aramid fabric tested at 102 m s⁻¹, respectively.

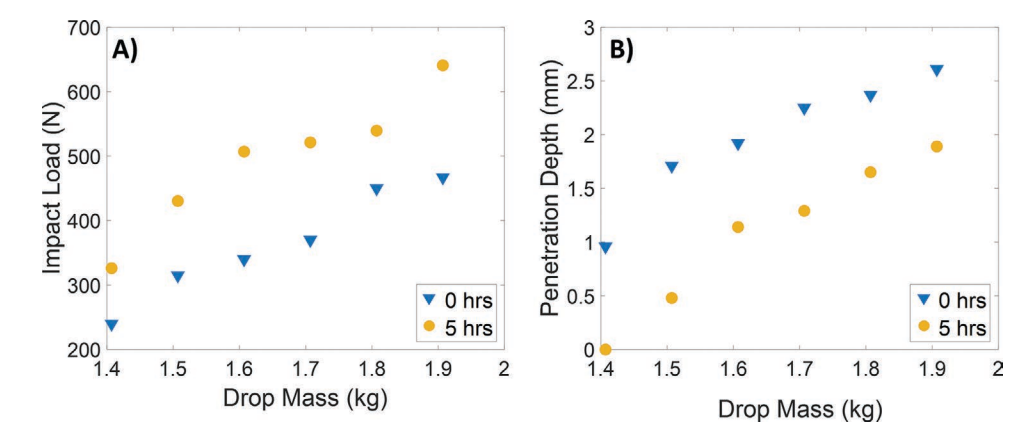


Figure 8. Quasistatic stab testing: A) Penetration depths of untreated and treated aramid fabric targets against spike impactor for different drop masses. B) Impact loads of untreated and treated aramid fabric targets against spike impactor for different drop masses. Comparison between untreated aramid fabrics and treated aramid fabrics after testing against spike impactor: C,D) damage to the front of untreated and treated aramid targets at a drop mass of 1.807 kg, respectively; E,F) damage to the back of untreated and treated aramid targets at a drop mass of 1.807 kg, respectively.

for adequate comparison. The drop height was fixed at 0.35 m. while the total drop mass was varied between 1.407 kg, which is the mass of the carriage unloaded, and 1.907 kg. The use of witness papers to measure depth of penetration was chosen over other approaches due to ease of implementation, rapid assessment of penetration depth, and high resolution given the thickness of each witness paper. Moreover, the witness paper approach avoids any inaccuracies in the depth of penetration measurements, as it accounts for any possible spring-back of the impactor by recording the initial penetration depth. The depth of penetration along with the impact load for each drop mass can be seen in Figure 8. An increasing trend in depth of penetration and impact load is observed in both untreated and treated fabrics with increasing drop mass. However, treated aramid fabrics display a significantly improved stab resistance compared to untreated aramid fabrics. For a drop mass of 1.407 kg, the fibrilized aramid fabric is able to prevent puncture, while untreated aramid fabric exhibits an ≈1 mm deep penetration. As drop mass is increased, treated aramid fabrics maintain their superior stab resistance, showing a maximum decrease of 230% in depth of penetration and a maximum increase of 110% in impact force. The decrease in depth of penetration is expected to be accompanied by an increase in impact load, as a larger portion of the kinetic impact energy is damped and absorbed by the aramid target, thus reducing the distance traveled by the impactor into the backing material. It should be noted that the maximum allowable depth of penetration without the likelihood of an injury is considered to be at 7 mm.[34] An inspection of the failure modes of untreated and treated aramid fabrics post-stabbing provides greater understanding of the role of the fibrilization treatment in the stab resistance reinforcement mechanism (Figure 9). For the same drop mass and height, untreated aramid targets display considerably more significant puncture damage than treated ones. Generally, spike impactors are able to penetrate aramid fabrics through intra- and intervarn slippage, resulting in little to no fiber tensile failure. The restricted mobility of neighboring fibers and tows in treated fabrics due to the improved interyarn friction provides higher resistance against stabbing by

preventing the spike from moving the filaments and penetrating. These results are further supported by quasistatic stab testing, where similar aramid targets were used. Figure 10 shows an 80% increase in supported stabbing load over a 15 mm penetration depth in treated aramid fabrics compared to that in untreated fabrics. While both fabrics are completely penetrated by the spike impactor, treated fabrics displayed a delay in complete target rupture and a significantly reduced stabbing compliance. This improvement in stab loading at slow rates is another indicator of the role of reduced yarn and fibers mobility in improving the stab resistance performance of aramid fibers. In conclusion, these results indicate the possibility of the fibrilization treatment providing significant stab

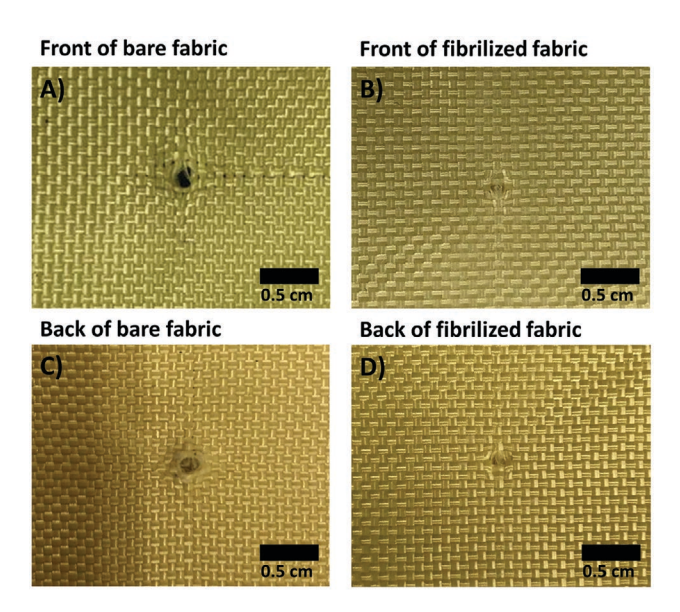


Figure 9. Comparison between untreated aramid fabrics and treated aramid fabrics after testing against spike impactor: A,B) damage to the front of untreated and treated aramid targets at a drop mass of 1.807 kg, respectively; C,D) damage to the back of untreated and treated aramid targets at a drop mass of 1.807 kg, respectively.

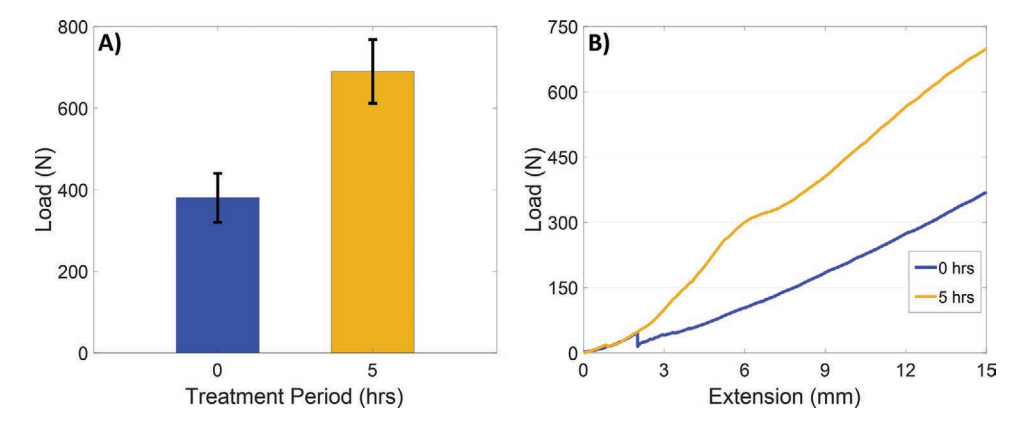


Figure 10. Quasistatic stab testing: A) maximum supported load by untreated and treated aramid fabric targets against spike impactor. B) Load-displacement curves of untreated and treated aramid fabric targets against spike impactor.

protection without any increase in weight or decrease in flexibility of the aramid fabric.

3. Conclusions

In summary, fibrilization was studied as an effective technique to enhance the pullout behavior and impact resistance of aramid (Kevlar KM2 Plus) fabrics. The treatment of aramid fibers in a strongly basic solution generates microscale-to-nanoscale fibrils on the surface of the fibers that help improve interfacial interaction between the neighboring yarns and fibers inside a woven fabric without degrading it. The intervarn friction of the fibrilized aramid fabric was significantly enhanced showing seven times higher pullout energy absorption, six times higher peak load, and extensional delays in pullout failure compared to untreated aramid fabrics. Through examination of the failure mode and load-displacement curves, mechanical interlocking between fibrilized fibers and tows was thought to be the primary reason for the enhanced pullout properties. The treated fibers also showed substantial increase in V_{50} velocity when subjected to impact testing in a four-side clamped configuration. These improvements to the impact response were explained by the considerable improvement in intervarn friction and reduced fabric deformation due to the limited mobility of both the yarn and the fiber. Finally, the decrease in yarn and fiber mobility also allowed treated fabrics to provide significant stab protection under both drop tower and quasistatic stab testing. Given the preservation of the strength, lightweight, and flexibility of the aramid fabric post-treatment, this rapid and low-cost fibrilization method possesses great potential to be integrated into the production of high-performance soft body armors.

4. Experimental Section

Fiber Fibrilization and Surface Characterization: Fibrilization of aramid fabric was performed using the method described by Nasser et al.^[45] Aramid unidirectional tape strips (Kevlar KM2 Plus, style 790 scoured, CS-800, received from JPS Composite Materials) were cleaned in acetone and ethanol to remove residual organic contaminants and sizing on the fabric surface and then dried at 100 °C for 12 h under vacuum. A solution consisting of 1.5 g of potassium hydroxide (KOH) (ACS certified; Fisher Scientific) in 500 mL of dimethyl sulfoxide (DMSO) (ACS certified; Fisher Scientific) was stirred for 30 min before adding the unidirectional tape to the beaker. The strips were soaked in the solution for 2, 5, 7, and 10 h, respectively. The treated strips were then washed with ethanol and dried at 80 °C under vacuum for 16 h. Untreated aramid fabric was also cleaned using the same process for comparison. The morphological changes on the fiber surfaces, before and after mechanical testing, were examined through SEM using a JEOL 7800 FLV field-emission scanning electron microscope.

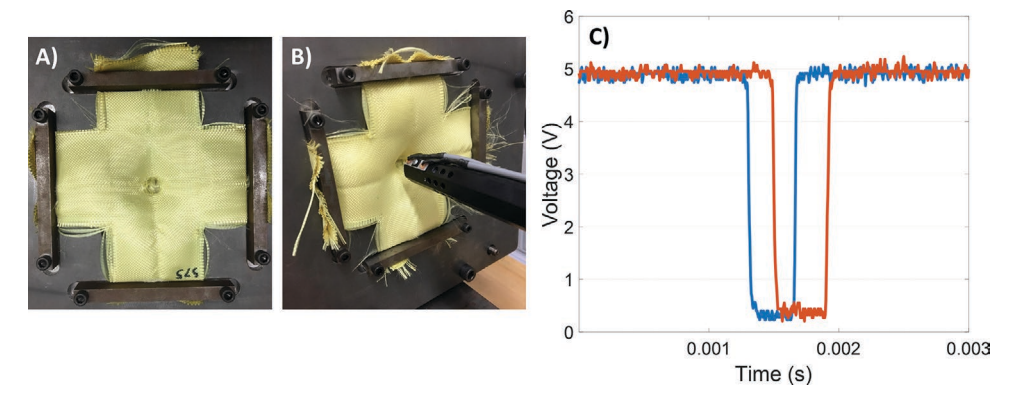


Figure 11. A) Cross-shaped, four-sided clamped aramid fabrics. B) Experimental setup using 0.25 in. distance between barrel and target. C) Photogates recorded signal as projectile exits the barrel.

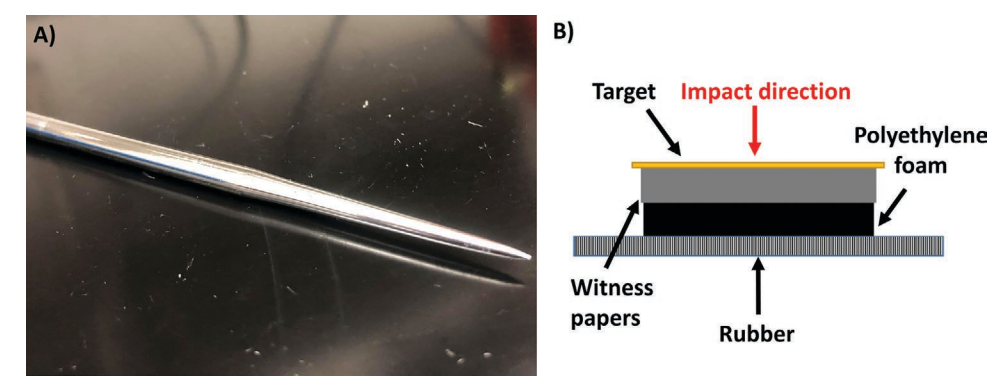


Figure 12. A) Spike impactor. B) Drop tower and quasistatic stabbing configuration.

Tensile Test: The strength of the treated fibers was tested through both textile fabric and single fiber tensile tests. Rectangular tensile specimens containing 20 yarns and having a gauge length of 75 mm were prepared from each set of untreated and treated aramid fabrics (statistics were calculated from 12 specimens for each set of fabric). Three plies of fabrics were bonded to each side of the fabric at the ends of the specimens by a high shear strength epoxy (Loctite 9430 Hysol) and were used as tabs to provide proper gripping during testing. All samples were tested in the weft (fill) direction using an Instron universal load frame (Model 5982) with a 100 kN load cell and at a cross-head speed of 300 mm min⁻¹. The specimens were strained until full failure before identification of the ultimate tensile strength and elongation of the fabrics. Single fiber tensile tests were performed according to ASTM C1557-03. Fiber samples were tested with a 12.7 mm gauge length at an extension rate of 16 $\mu m s^{-1}$ on the same Instron load frame equipped with a static load cell (Model 2530) with a 5 N capacity.

Tow Pullout Testing: To investigate the effect of the fibrilization treatment on the ballistic response of the aramid fabrics, the sliding friction between tows was quantified by the tow pullout test under controlled transverse tension. The test was conducted on a customdesigned tow pullout setup similar to that described by Hwang et al. (Figure 3).^[41] Aramid fabric samples of ≈165 mm (6.5 in.) in width and 127 mm (5 in.) in length were prepared by manually removing the transverse yarns to provide a 114 mm overhang of free yarn, while the remaining fabric, consisting of 20 transverse tows, was clamped in the direction of the pull and was kept constant for all experiments. The treated fabric patches were clamped between a fixed column and an adjustable link, where a lead screw was used to adjust the clamping distance and thus apply lateral tension to the fabric. A 445 N (100 lb) load cell was placed between a plate at the end of the lead screw and the second fixed column and was used in compression mode to measure the applied transverse tensile force. The tow pullout tests were performed by pulling a single tow from the taught, preloaded fabric using an Instron 5982 machine equipped with a 100 kN load cell, at a pullout rate of 50 mm min⁻¹ and an applied transverse tension of 100 N. For each fabric sample, tabs were added to the free end of seven tows for proper gripping, having a spacing of ten tows between tabbed tows. Finally, all seven tow samples were pulled in the warp direction only, as marked in Figure 3A.

High Velocity Impact Test: The ballistic performance of the fibrilized aramid fabric was further studied through ballistic impact tests performed using a custom-designed gas gun setup as described in the study of Stenzler. [48] The compressed air driven ballistic setup was instrumented for accurate measurement of projectile's impact velocity. The velocity of the projectile was obtained by recording the time required for it to block the incident light by traveling between two photoresistors placed 19.05 mm (3/4 in.) apart at the end of the barrel. A blunt 4130 alloy steel projectile (hemispherical face) with a mass of 29 g and a diameter of 11.4 mm was used to impact the fabric targets consisting of three cross-shaped aramid fabric plies with a square target area of 7.8 × 7.8 cm². The samples were clamped from all four sides

using a steel plate with recessed bars as shown in **Figure 11**A,B. The applied torques to the steel plates and bars screws were controlled using a torque-wrench to ensure uniform clamping and prevent any target slippage during impact. The impact of the projectile on the target surface was designed for zero degrees of obliquity. A clay trap was also placed 2 in. behind the target and was examined for penetration after each firing of a projectile. For each set of aramid fabric, 12 targets were shot and the V_{50} BL(P) ballistic performance was obtained by taking the arithmetic mean of the three highest nonpenetrating and the three lowest complete penetrating impact velocities into the clay trap.

Stab Testing: The influence of fibrilization treatment on the stab resistance of aramid fabrics was also examined using drop tower testing. A "spike" impactor (Figure 12A) was rigidly mounted to a crosshead in a conventional, rail guided drop tower, while aramid stab targets were placed on top of a multilayer backing (Figure 12B). Each stab target consisted of eight aramid fabric plies positioned on top of 200 witness papers followed by a 6 mm thick layer of rubber. The targets were then fixed during testing using Velcro nylon straps. Targets were impacted by loading the crosshead with weights up to a predetermined mass and dropping it from a fixed height. The velocity of the crosshead was obtained using a Keyence LJ-V7000 series laser profilometer which tracks the vertical motion of the carriage. Impact loads were measured using a dynamic load cell mounted to the impactor. The depth of penetration was evaluated using the number of witness papers penetrated by the impactor and validated using the measurements from the displacement laser. The full set of testing conditions can be found in Table 3. Testing was performed on both untreated and aramid fabrics fibrilized for 5 h. It should be noted that the same number of plies was used for each set of fabrics as treatment resulted in no significant changes to the aerial density of the aramid fabric.

Quasistatic stab tests were also performed by mounting a spike impactor to the upper grip of an Instron 5982 machine equipped with a 100 kN load cell, with the target placed below the impactor and on top of the same multilayered backing used during the drop tower tests (Figure 12B). The impactor was then pushed into the target at a rate of 5 mm min $^{-1}$ to a total depth of 15 mm while recording load versus displacement measurements.

Table 3. Conditions for drop tower stab testing.

Drop mass [kg]	Drop height [m]	Theoretical impact velocity $[m\ s^{-1}]$	Theoretical impact energy [J]
1.407	0.35	2.62	4.831
1.507	0.35	2.62	5.174
1.607	0.35	2.62	5.517
1.707	0.35	2.62	5.861
1.807	0.36	2.62	6.204
1.907	0.35	2.62	6.376

www.advancedsciencenews.com



www.advmatinterfaces.de

Acknowledgements

The authors gratefully acknowledge financial support for this research from the Army Research Office (Contract #W911NF-18-1-0061).

Conflict of Interest

The authors declare no conflict of interest.

Keywords

aramid fabric, ballistic, fibrilization, impact response, interyarn friction, stab resistance

Received: May 19, 2019 Revised: June 28, 2019 Published online: August 6, 2019

- [1] A. Bhatnagar, Lightweight Ballist. Compos. 2016.
- [2] A. Helliker, Lightweight Ballist. Compos. 2016, 87.
- [3] N. K. Naik, P. Shrirao, Compos. Struct. 2004, 66, 579.
- [4] D. Gay, S. Hoa, S. Tsai, Composite Materials, CRC Press, Boca Raton, FL 2002.
- [5] K. K. Chawla, Composites 1989, 20, 286.
- [6] A. Tabiei, G. Nilakantan, Appl. Mech. Rev. 2008, 61, 010801.
- [7] P. M. Cunniff, presented at 18th Int. Symp. Ballistics, San Antonio, TX. November 1999.
- [8] L. Bin Tan, K. M. Tse, H. P. Lee, V. B. C. Tan, S. P. Lim, Int. J. Impact Eng. 2012, 50, 99.
- [9] E. Lewis, D. J. Carr, Lightweight Ballist. Compos. 2016, 217.
- [10] L. Bracamonte, R. Loutfy, I. K. Yilmazcoban, S. D. Rajan, Lightweight Ballist. Compos. 2016, 349.
- [11] W. Li, D. Xiong, X. Zhao, L. Sun, J. Liu, Mater. Des. 2016, 102, 162.
- [12] R. Gadow, K. von Niessen, Int. J. Appl. Ceram. Technol. 2006, 3,
- [13] J. Ting, D. Roylance, C. H. Chi, presented at 25th Int. SAMPE Tech. Conf., Philadelphia, PA, 1993.
- [14] Improved Barriers to Turbine Engine Fragments: Interim Report II,
- [15] Chitrangad (E I du Pont de Nemours and Co.), US5187003A, 1991.
- [16] C. Lim, V. B. Tan, C. Cheong, Int. J. Impact Eng. 2002, 27, 577.
- [17] P. M. Cunniff, Text. Res. J. 1992, 62, 495.
- [18] Y. Rao, R. J. Farris, J. Appl. Polym. Sci. 2000, 77, 1938.
- [19] J. M. Pereira, G. D. Roberts, D. M. Jr. Revilock, Elevated Temperature Ballistic Impact Testing of PBO of Kevlar Fabrics for Application in Supersonic Jet Engine Fan Containment Systems 1997.

- [20] K. Pandya, C. V. S. Kumar, N. Nair, P. Patil, N. Naik, Int. J. Damage Mech. 2015, 24, 471.
- [21] D. J. Carr, J. Mater. Sci. Lett. 1999, 18, 585.
- [22] B. J. Briscoe, F. Motamedi, Wear 1992, 158, 229.
- [23] B. J. Briscoe, F. Motamedi, Text. Res. J. 1990, 60, 697.
- [24] R. L. Gorowara, W. E. Kosik, S. H. McKnight, R. L. McCullough, Composites, Part A 2001, 32, 323.
- [25] E. D. LaBarre, X. Calderon-Colon, M. Morris, J. Tiffany, E. Wetzel, A. Merkle, M. Trexler, J. Mater. Sci. 2015, 50, 5431.
- [26] W. Lee, J. U. Lee, J.-H. Byun, Compos. Sci. Technol. 2015, 110, 53.
- [27] B. A. Patterson, H. A. Sodano, ACS Appl. Mater. Interfaces 2016, 8, 33963.
- [28] H. Qian, A. Bismarck, E. S. Greenhalgh, M. S. P. Shaffer, Compos. Sci. Technol. 2010, 70, 393.
- [29] L. Dischler, (Milliken Research Corp.), US5225241A, 1992.
- [30] J. M. R.-P. Chitrangad, (E I du Pont de Nemours and Co.), EP0623180B1, 1992.
- [31] S. Bazhenov, J. Mater. Sci. 1997, 32, 4167.
- [32] S. Rebouillat, (Stephenson Group Ltd.), US5443896A, 1993.
- [33] Y. S. Lee, E. D. Wetzel, N. J. Wagner, J. Mater. Sci. 2003, 38, 2825.
- [34] R. G. Egres, M. J. Decker, C. J. Halbach, Y. S. Lee, J. E. Kirkwood, K. M. Kirkwood, N. J. Wagner, E. D. Wetzel, *Transformational Science and Technology for the Current and Future Force*, World Scientific, Singapore 2006, pp. 264–271.
- [35] A. Gawandi, E. T. Thostenson, J. W. Gilllespie, J. Mater. Sci. 2011, 46, 77.
- [36] V. Obradović, D. B. Stojanović, R. Jančić-Heinemann, I. Živković, V. Radojević, P. S. Uskoković, R. Aleksić, J. Eng. Fibers Fabr. 2014, 9.
- [37] Y. Lin, G. Ehlert, H. A. Sodano, Adv. Funct. Mater. 2009, 19, 2654.
- [38] M. H. Malakooti, H.-S. Hwang, H. A. Sodano, ACS Appl. Mater. Interfaces 2015, 7, 332.
- [39] U. Galan, Y. Lin, G. J. Ehlert, H. A. Sodano, Compos. Sci. Technol. 2011, 71, 946.
- [40] H.-S. Hwang, M. H. Malakooti, H. A. Sodano, Composites, Part A 2015, 76, 326.
- [41] H.-S. Hwang, M. H. Malakooti, B. A. Patterson, H. A. Sodano, Compos. Sci. Technol. 2015, 107, 75.
- [42] M. H. Malakooti, H.-S. Hwang, N. C. Goulbourne, H. A. Sodano, Composites, Part B 2017, 127, 222.
- [43] M. H. Malakooti, Z. Zhou, J. H. Spears, T. J. Shankwitz, H. A. Sodano, Adv. Mater. Interfaces 2016, 3, 1500404.
- [44] G. J. Ehlert, Y. Lin, U. Galan, H. A. Sodano, J. Solid Mech. Mater. Eng. 2010, 4, 1687.
- [45] J. Nasser, J. Lin, H. Sodano, J. Appl. Phys. 2018, 124, 045305.
- [46] G. Nilakantan, M. Keefe, E. D. Wetzel, T. A. Bogetti, J. W. Gillespie, Compos. Sci. Technol. 2012, 72, 320.
- [47] R. B. Seymour, Applications of Polymers, Springer US, Boston, MA 1988, p. 15.
- [48] J. S. Stenzler, *Doctoral Thesis*, Virginia Polytechnic Institute and State University, Blacksburg, VA 2009.